

Structure Activity of 3-Aryl-1,3-diketo-Containing Compounds as HIV-1 Integrase Inhibitors¹

Godwin C. G. Pais,[†] Xuechun Zhang,[†] Christophe Marchand,[‡] Nouri Neamati,[‡] Kiriana Cowansage,[‡] Evguenia S. Svarovskaia,[§] Vinay K. Pathak,[§] Yun Tang,[†] Marc Nicklaus,[†] Yves Pommier,[‡] and Terrence R. Burke, Jr.^{*,†}

Laboratory of Medicinal Chemistry, Laboratory of Molecular Pharmacology, and HIV Drug Resistance Program, Center for Cancer Research, National Cancer Institute, National Institutes of Health, Frederick, Maryland 21702-1201

Received January 24, 2002

The 4-aryl-2-hydroxy-4-oxo-2-butenic acids and their isosteric tetrazoles are among an emerging class of aryl β -diketo (ADK)-based agents which exhibit potent inhibition of HIV-1 integrase (IN)-catalyzed strand transfer (ST) processes, while having much reduced potencies against 3'-processing (3'-P) reactions. In the current study, L-708,906 (**10e**) and 5CITEP (**13b**), which are two examples of ADK inhibitors that have been reported by Merck and Shionogi pharmaceutical companies, served as model ADK leads. Structural variations to both the "left" and "right" sides of these molecules were made in order to examine effects on HIV-1 integrase inhibitory potencies. It was found that a variety of groups could be introduced onto the left side aryl ring with maintenance of good ST inhibitory potency. However, introduction of carboxylic acid-containing substituents onto the left side aryl ring enhanced 3'-P inhibitory potency and reduced selectivity toward ST reactions. Although both L-708,906 and 5CITEP show potent inhibition of IN in biochemical assays, there is a disparity of antiviral activity in cellular assays using HIV-1-infected cells. Neither 5CITEP nor any other of the indolyl-containing inhibitors exhibit significant antiviral effects in cellular systems. Alternatively, consistent with literature reports, L-708,906 does provide antiviral protection at low micromolar concentrations. Interestingly, several analogues of L-708,906 with varied substituents on the left side aryl ring, while having good inhibitory potencies against IN in extracellular assays, are not antiviral in whole-cell systems.

Introduction

Human immunodeficiency virus type 1 (HIV-1) encodes three enzymes which are required for viral replication: reverse transcriptase, protease, and integrase (IN). Although drugs targeting reverse transcriptase and protease are in wide use and have shown effectiveness particularly when employed in combination,² toxicity and development of resistant strains have limited their usefulness.³ Impetus, therefore, exists for the discovery of new agents directed against alternate sites in the viral life cycle. IN has emerged as an attractive target, because it is necessary for stable infection⁴ and homologous enzymes are lacking in the human host. The function of IN is to catalyze integration of proviral DNA, resulting from the reverse transcription of viral RNA, into the host genome. This is achieved in a stepwise fashion by endonucleolytic processing of proviral DNA within a cytoplasmic preintegration complex (termed 3'-processing or "3'-P"), followed by translocation of the complex into the nuclear compartment where integration of 3'-processed proviral DNA into host DNA occurs in a "strand transfer" (ST) reaction. Although numerous agents potently inhibit 3'-P and ST

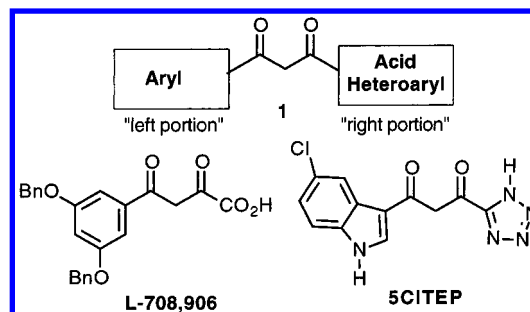


Figure 1. General aryl diketo-based inhibitor (**1**) with two recently reported examples.

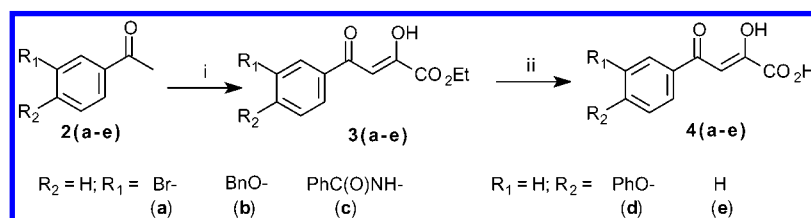
in extracellular assays that employ recombinant IN and viral long terminal repeat oligonucleotide sequences,⁵ often such inhibitors lack inhibitory potency when assayed using fully assembled preintegration complexes⁶ or fail to show antiviral effects against HIV-infected cells.⁷ Recently, however, a class of IN inhibitors has emerged, typified by an aryl β -diketo motif (ADK (**1**), Figure 1). Variations of this structural theme have been utilized by Shionogi^{8,9} and Merck^{10–12} pharmaceutical companies to prepare inhibitors (for example, 5CITEP¹³ and L-708,906,¹⁴ Figure 1), some of which potently block integration in extracellular assays and exhibit good antiviral effects against HIV-infected cells. Further studies have indicated that, unlike numerous other IN inhibitors whose antiviral effects can be attributable to non-integrase-dependent phenomena,^{15,16} members of the ADK family disrupt viral

* To whom correspondence should be addressed: Laboratory of Medicinal Chemistry, Center for Cancer Research, NCI-Frederick, P.O. Box B, Bldg. 376 Boyles St., Frederick, MD 21702-1201. Tel: (301) 846-5906. Fax: (301) 846-6033. E-mail: tburke@helix.nih.gov.

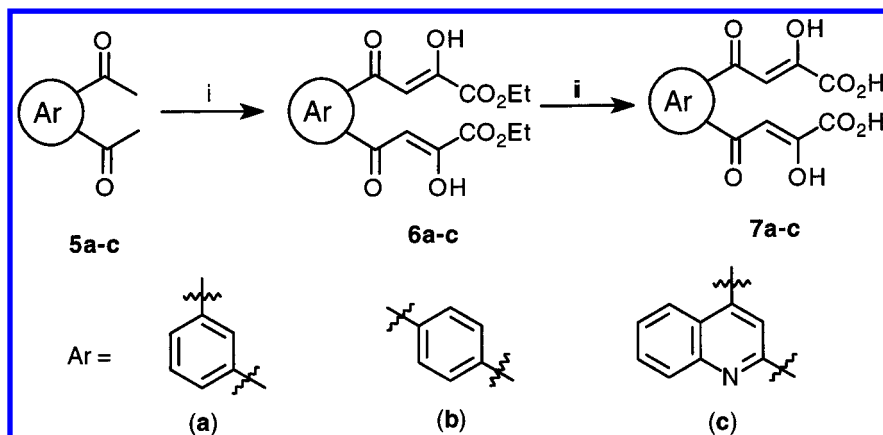
[†] Laboratory of Medicinal Chemistry.

[‡] Laboratory of Molecular Pharmacology.

[§] HIV Drug Resistance Program.

Scheme 1^a

^a (i) $(\text{CO}_2\text{Et})_2$, NaH, toluene (60 °C, 3 h) (for **2e**, 110 °C, 1 h); (ii) 1 N NaOH, dioxane (rt, 1 h).

Scheme 2^a

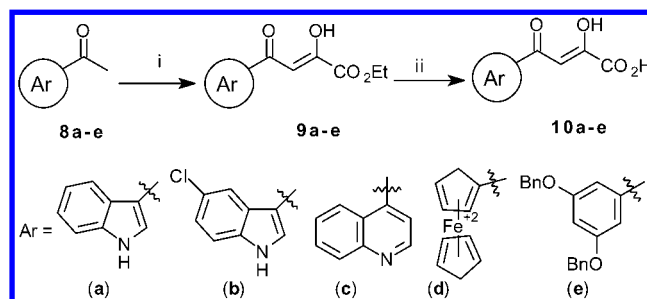
^a (i) $(\text{CO}_2\text{Et})_2$, NaOEt, THF (rt, 3 h; 50 °C, 18 h); (ii) KOH, EtOH (reflux 15 h) or 1 N NaOH, THF-EtOH (1:1) (rt 1 h) for **6c**.

infectivity in a manner consistent with inhibition of integration.^{14,16,17} Finally, evidence has been presented that at least some ADK-based inhibitors show selective inhibition of the ST reaction relative to the 3'-P step and may function by competing with host DNA in binding to the IN-proviral DNA complex.^{14,18,19} Although ADK-motifs currently present some of the most promising starting points for inhibitor development,²⁰⁻²² few structure-activity relationship (SAR) studies have been reported on this genre of compounds.²³ Accordingly, herein is reported an examination of the structural features of the ADK family as they relate to IN inhibitory potency and selectivity.

Synthesis

4-Aryl-2-hydroxy-4-oxo-2-butenic Acids. Synthesis of 4-aryl-4-oxo-2-hydroxy-2-butenic acids occurred with the oxalation of the corresponding aryl ketones in the presence of base, followed by either alkaline or acidic hydrolysis (Schemes 1-3).^{23,24} For analogues containing a phenyl aryl portion and a single 2,4-dioxobutanoyl side chain (**4a-e**), synthesis according to the literature procedures provided aryl ketones (**2a-e**). These were coupled with diethyl oxalate in the presence of NaH to give intermediate ethyl esters (**3a-e**) which were converted to free acids (Scheme 1). Among the methods investigated for ethyl ester hydrolysis, aqueous 1 N NaOH in dioxane proved to be the most effective.

Synthesis of bis-[4-(2-hydroxy)-4-oxo-2-butenic acid]-containing compounds **7a-c** was achieved in a similar fashion by coupling bis-(methyl ketones) **5a-c** with diethyl oxalate in the presence of NaOEt,²⁵ with hydrolysis of the resulting bis-(ethyl esters) **6a-c** being subsequently carried out in the presence of KOH in refluxing EtOH (Scheme 2). Note that for product **7c**,

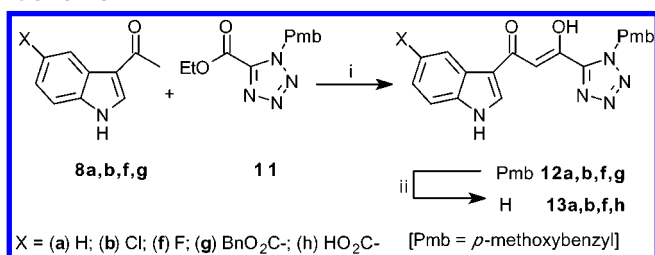
Scheme 3^a

^a (i) $(\text{CO}_2\text{Et})_2$, NaOEt, THF (rt, 3 h; 50 °C, 18 h) or NaH, toluene (for **9d**, 110 °C, 1 h); (ii) KOH, EtOH (reflux 15 h) or 1 N NaOH, THF-EtOH (1:1) (rt, 1 h) for **10c,d**.

milder conditions were employed (1 N NaOH in THF-EtOH at room temperature).²³ Heteroaryl and ferrocene-containing acids **10a-d** and 3,5-dibenzyloxy derivative **10e** were prepared in a similar fashion (Scheme 3).

4-Aryl-3-hydroxy-4-oxo-3-(1H-tetrazol-5-yl)-propanone Derivatives (12, 13, 15, and 16). Acetyl indoles **8a,b,f,g** were coupled with **11**²⁶ in the presence of LHMDS to provide *p*-methoxybenzyl-protected tetrazoles **12a,b,f,g**. The final products **13a,b,f,h** were obtained by the removal of the tetrazole protection using TFA with ethanedithiol as a scavenger (Scheme 4). For **13h**, hydrogenolytic cleavage of the benzyl ester was accomplished prior to treatment with TFA. Tetrazole **14** was synthesized from 3,5-dimethoxybenzyl bromide in a fashion similar to the synthesis of **11**. Treatment of **8e** with **11** gave the protected tetrazole derivative **16b**. Attempts to selectively remove the *p*-methoxybenzyl group of **16b** were not successful (Scheme 5).

Evaluation of Antiviral Activity. A single-cycle replication assay was utilized to measure the antiviral activity of selected compounds, wherein an envelope-deficient HIV-1-based retroviral vector containing the

Scheme 4^a

^a (i) LHMDs, THF (−20 °C, 2 h, −78 °C to rt, 1 h, rt, 2 h); (ii) TFA, ethane dithiol–H₂O (1:1) (rt, 20 h) [for **12g**, H₂/Pd–C, THF then (ii)]. Note: For **13g**, X = HO₂C.

firefly luciferase reporter gene (pNluc) was cotransfected into 293T cells with vesicular stomatitis virus G glycoprotein (VSV-G) expressing plasmid (CMV-VSV-G). Virus harvested from transfected cells was used to infect target cells in the presence or absence of the compounds tested. The ability of compounds to inhibit viral replication was measured by determining the amount of luciferase activity in the infected cells. Additionally, concentrations of compounds that resulted in 50% inhibition of HIV-1 infection (IC₅₀ values) were determined for compounds that displayed antiviral activity at a concentration of 25 μM (Table 2). For these latter determinations, single-cycle HIV-1 replication assays were performed in the presence of a series of inhibitor concentrations (0.05, 0.5, 5, and 50 μM). To determine a relative inhibition of HIV-1 infection at each concentration, luciferase activity of each sample was normalized to the untreated control.

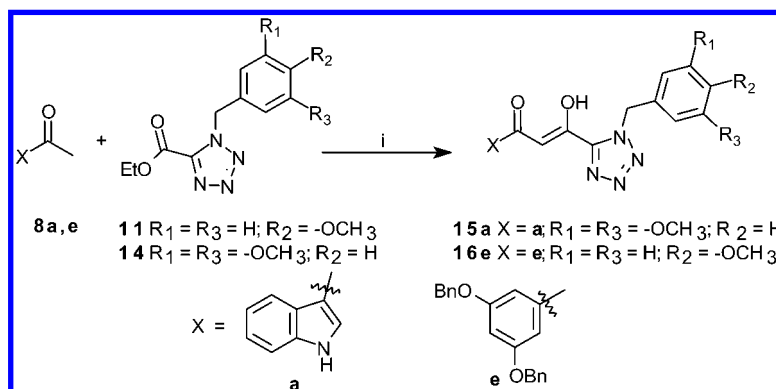
Molecular Modeling. A model of the IN core complexed with viral DNA was initially constructed utilizing all available experimental evidence and refined by molecular dynamics simulation.²⁷ This hypothetical model was intended to represent IN immediately following the first catalytic reaction (3'-processing). The model was refined by placing two Mg²⁺ ions into the active site, which is a cleft formed partly by both the protein and DNA. The location of these metal ions was based on experimental evidence and the hypothesis that a second metal ion was likely to be carried into the HIV-1 IN active site by viral DNA binding.²⁸ One Mg²⁺ ion coordinated with the carboxyl groups of Asp64 and Asp116. The other metal ion was bound to the carboxyl group of Glu152, the carbonyl group of Asn155, and the phosphate group of the last adenosine of the viral DNA (proximal to the G–T nucleotides which are cut during

the 3'-processing reaction). The distance between the two Mg²⁺ ions remained constant throughout the molecular dynamics simulation at approximately 7 Å.²⁷

Results and Discussion

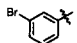
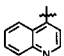
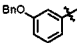
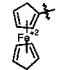
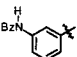
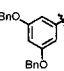
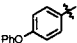
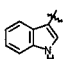
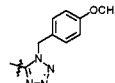
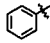
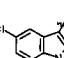
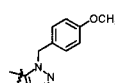
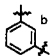
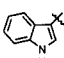
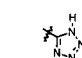
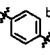
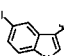
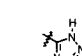
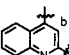
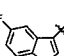
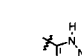
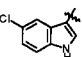
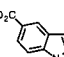
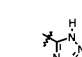
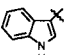
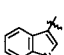
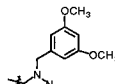
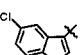
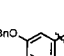
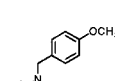
Our interest in the ADK class of IN inhibitors began with the disclosure of the X-ray crystal structure of 5CITEP (**13b**) complexed to the catalytic D64, D116, and E152 residues of the IN core domain.¹³ This provided preliminary evidence that ADK-containing agents may potentially afford promising leads for the development of IN inhibitors.²² Such expectations were supported by subsequent reports that structurally related ADK-containing compounds exhibit potent IN inhibition and elicit good antiviral effects in HIV-infected cells.^{14,18} Although both Shionogi's 5CITEP and Merck's ADK-based inhibitors share a common β-diketopropyl central chain, they differ in their "left" and "right" portions (Figure 1). Since only limited structure–activity or synthetic studies of these inhibitors have been reported,²³ the current study was undertaken to examine aspects of both the left and right portions of the molecules.

Inhibitory Potencies in HIV-1 Integrase Assays: Modifications to the Left Side of 5CITEP. In the report of 5CITEP (**13b**) complexed with the IN catalytic domain, inhibitory data against IN were minimal and did not include antiviral potency in HIV-infected cells.¹³ Therefore, this previously disclosed inhibitor was prepared in order to determine its inhibitory profile against 3'-P and ST as well as its antiviral potency in HIV-infected cells. Additionally, the importance of the chloro substituent at the indolyl 5-position was examined through the preparation of agents (**13a**, **13f**, and **13h**) whose functionalities varied at the 5-position. Inhibitory values measured in an extracellular integrase assay are shown in Table 1. Antiviral potencies in HIV-infected cells were also determined (Table 2) for analogues exhibiting IC₅₀ ≤ 10 μM in this assay. We found that 5CITEP (**13b**) exhibits potent inhibition of ST, while it is much less effective for inhibiting 3'-P (approximately 50-fold). Substitution of the 5-Cl with hydrogen (**13a**) decreases 3'-P inhibitory potency, whereas fluorine (**13f**) exhibits 3'-P inhibitory potency equivalent to that of the parent chlorine. Substitution with either hydrogen or fluorine has little effect on ST inhibitory potency. Replacement of the 5-Cl with a carboxyl group (**13h**) significantly decreases the

Scheme 5^a

^a (i) LHMDs, THF −20 °C, 2 h, −78 °C to rt, 1 h; rt 2 h.

Table 1. Inhibitory Potencies As Measured in an Extracellular HIV-1 Integrase Assay^a

General Structure									
IC ₅₀ (μM)					IC ₅₀ (μM)				
No.	X	Y	3'-P	ST	No.	X	Y	3'-P	ST
4a		-CO ₂ H	>100	2.0, 3.0	10c		-CO ₂ H	>100	>100
4b		-CO ₂ H	65, 100	0.35 ± 0.13 (n = 3)	10d		-CO ₂ H	11.5	0.81
4c		-CO ₂ H	>100	35	10e		-CO ₂ H	>1000	0.48 ± 0.08 (n = 4)
4d		-CO ₂ H	>100	7.8, 15	12a			>100	>100
4e		-CO ₂ H	>100	24.2, 25.0	12b			>100	34
7a		-CO ₂ H	7.8 ± 2.2 (n = 3)	1.83 ± 0.32 (n = 3)	13a			>100	1.9, 2.0
7b		-CO ₂ H	7.2, 7.5	1.28 ± 0.38 (n = 3)	13b			35	0.65 ± 0.19 (n = 4)
7c		-CO ₂ H	82	6.5 ± 0.81 (n = 3)	13f			79	1.8
9b		-CO ₂ Et	>100	6.9	13h			40	40
10a		-CO ₂ H	>100	1.43 ± 0.15 (n = 3)	15a			>100	>100
10b		-CO ₂ H	65	0.52 ± 0.10 (n = 3)	16b			>100	>100

^a Values were determined as described in the Experimental Section. ^b Structures as described in Scheme 2.**Table 2.** Antiviral Data for Selected Inhibitors As Measured in a Single-Cycle Replication Assay Using Envelope-Deficient HIV-1^a

% control				% control			
no.	experiment 1	experiment 2	comment	no.	experiment 1	experiment 2	comment
4a	92	103	IC ₅₀ = 0.6 μM	10a	1	0	cytotoxic ^b
4b	14	25		10b	91	85	cytotoxic ^b IC ₅₀ = 2.3 μM
4d	261	208		10d	36	69	
7a	98	95		10e	7	19	
7b	133	128		13a	116	87	
7c	61	94		13b	125	69	
9b	104	63		13f	65	70	

^a Compounds exhibiting ST IC₅₀ values of ≤10 μM in extracellular HIV integrase assays (Table 1) were selected for evaluation and tested initially at a concentration of 25 μM as described in the Experimental Section. Compounds **4b** and **10e**, which achieved ≥50% inhibition at 25 μM, were examined over a concentration range to determine the IC₅₀ values. ^b Cytotoxicity was determined by visual inspection of cells.

inhibitory potency against ST while approximately doubling potency against 3'-P. This resulted in a complete loss of ST/3'-P selectivity.

Modifications to the Right Side. L-708,906 (**10e**) and 5CITEP (**13b**), while sharing a common 1,3-diketone moiety, differ both in their left aryl portions

and in their right side functionality. The former possesses a carboxylic acid group, and the latter possesses a tetrazole group. It is known that tetrazoles can serve as isosteric replacements for carboxyl groups.^{29,30} However, the biological effects of such an interchange are complicated in the ADK class of IN inhibitors due to the potential importance of tetrazole nitrogens for the binding of 5CITEP to the enzyme as indicated by X-ray crystallography.¹³ Therefore, replacement of the tetrazole group with carboxyl functionality was examined for both 5CITEP (**13b**) and its des-chloro congener (**13a**). The resulting analogues (**10b** and **10a**, respectively) exhibited little change in either 3'-P or ST inhibition potencies (Table 1). The blockade of the carboxyl hydroxyl of the 5CITEP analogue **10b** by conversion to its ethyl ester (**9b**) was accompanied by maintenance of the significant ST inhibitory potency and selectivity over 3'-P. This indicates that an acidic proton may not be required for ST inhibitory potency. The fact that a blockade of acidic protons of tetrazole-containing analogues (**13a,b**), with either 4-methoxybenzyl groups (**12a,b**) or a 3,5-dimethoxybenzyl group (**15a**), resulted in a significant loss of ST inhibitory potency may be due to steric hindrance rather than a loss of acidic protons.

Analogues of L-708,906. A second class of ADK-containing inhibitors, as exemplified by Merck's L-708,906¹⁴ (Figure 1, designated as **10e** in Table 1), is characterized by a carboxyl group on the right side and multiple aryl rings on the left side. The biological properties of this class have been more extensively detailed than those of 5CITEP. It has been shown that L-708,906 potently inhibits HIV-1 IN-catalyzed ST processes while having little effect on 3'-P catalysis.¹⁸ Inhibition of viral replication in HIV-1-infected cells by L-708,906 is achieved at low micromolar concentrations, and resistant viral strains bear mutations which map to integrase. These mutations include M154I, S153Y, and T66I which are proximal to active site Glu152 and Asp64 residues, respectively.¹⁸

Further studies, using related analogues bearing pyrrole-based left side groups, provide evidence that this class of ADK inhibitor may function by competing for host DNA binding to the IN-viral DNA complex.¹⁴ Finally, a structure-activity investigation based on a pyrrole-containing lead ADK inhibitor has presented a focused examination of specific aspects of this family.²³ Our current study is complementary to this latter report in exploring a wider range of structural diversity in the left side portion of the ADK theme.

Consistent with literature findings,¹⁸ L-708,906 exhibited potent inhibition of ST with no effect on 3'-P up to 1000 μ M (**10e**, Table 1). Removal of one benzyloxy group (compound **4b**) resulted in a slight increase in ST inhibitory potency and some loss of selectivity relative to 3'-P. Removal of the remaining 3-benzyloxy group (**4e**) gave a greater than 50-fold loss of ST inhibitory potency, while introduction of a 3-bromo substituent (**4a**) gave a significant restoration of potency. The importance of functionality at the aryl 3-position was shown further when the replacement of the benzyloxy group in **4b** with a benzoylamino group (**4c**) reduced ST inhibitory potency by approximately 100-fold. Aryloxy substituents at other sites, such as the 4-position (**4d**), also reduced ST inhibitory potency. Replacement of the unsubstituted

phenyl ring of **4e** with a 4-quinolyl ring (**10c**) resulted in a dramatic loss of inhibitory potency. This is in contrast to the good ST inhibitory potency shown by the indolyl analogue **10a**.

Although above outlined modifications to L-708,906 (**10e**) affected the potency of ST inhibition, the selectivities of ST versus 3'-P were maintained. In a further set of analogues, additional 2,4-diketobutyric acid groups were added at the 3- or 4-position of the left side aryl ring (**7a** or **7b**, respectively). Interestingly, while ST inhibitory potency was largely unaffected, these bifunctional analogues displayed enhanced 3'-P inhibitory potencies, such that selectivity toward ST was very much reduced. Adding a second diketo acid side chain to quinolyl-containing **10c**, which was essentially inactive, gave **7c** which displayed greatly restored inhibitory potency. The loss of ST to 3'-P selectivity by these bifunctional analogues differentiates them from other ADK inhibitors which are generally characterized by high ST selectivity. Potential mechanistic considerations of bis-diketo acid inhibitors are discussed elsewhere.¹⁹

Antiviral Effects. While potent inhibition in extracellular IN assays has been reported for an extensive array of compounds, demonstration of antiviral effects against HIV-infected cells for agents that exhibit good potency in these extracellular enzyme assays has been more elusive. The ability of certain ADK-based IN inhibitors to elicit potent antiviral effects by mechanisms consistent with intracellular inhibition of IN has set this class apart.^{14,16,17}

A total of 12 compounds were tested for their ability to inhibit HIV-1 infection. The compounds were preselected for antiviral evaluation based on the ST inhibitory potencies (IC_{50} values $\leq 10 \mu$ M) as listed in Table 1. It should be noted that Mn^{2+} rather than Mg^{2+} was utilized for in vitro assays, because the soluble mutant integrase enzyme employed functions more efficiently with this metal ion than with Mg^{2+} . Although in vivo the cation used by integrase is unclear, it may be Mg^{2+} , and for this reason, IC_{50} values obtained using Mn^{2+} may not accurately reflect in vivo inhibition. Initially, the compounds were tested at 25 μ M concentrations with the results being summarized in Table 2. L-708,906 (**10e**) was used as a control because of its known ability to inhibit HIV-1 integration in vitro and in vivo.^{17,18} In the current assay, **10e** at 25 μ M reduced HIV-1 infection to an average of 13% of the untreated control, indicating that this compound was active in inhibiting HIV-1 replication. For compounds exhibiting antiviral activity at 25 μ M concentrations (**4b** and **10e**), further experiments were conducted to determine antiviral IC_{50} values. These experiments indicated that IC_{50} values for **4b** and **10e** were 0.6 and 2.3 μ M, respectively. The IC_{50} value for **10e** (2.3 μ M) was very similar to the previously reported IC_{50} value (2.5 μ M).¹⁸ Interestingly, although **4b** is structurally related to **10e**, it exhibits a lower IC_{50} value (0.6 μ M) suggesting that it may be more effective at inhibiting HIV-1 replication than **10e**. Two compounds (**10a** and **10d**) displayed deleterious effects on cell viability as determined by visual examination of cell cultures following incubation with these compounds during infection. For these agents, reduction in luciferase activity was most likely due to cytotoxicity (Table 2).

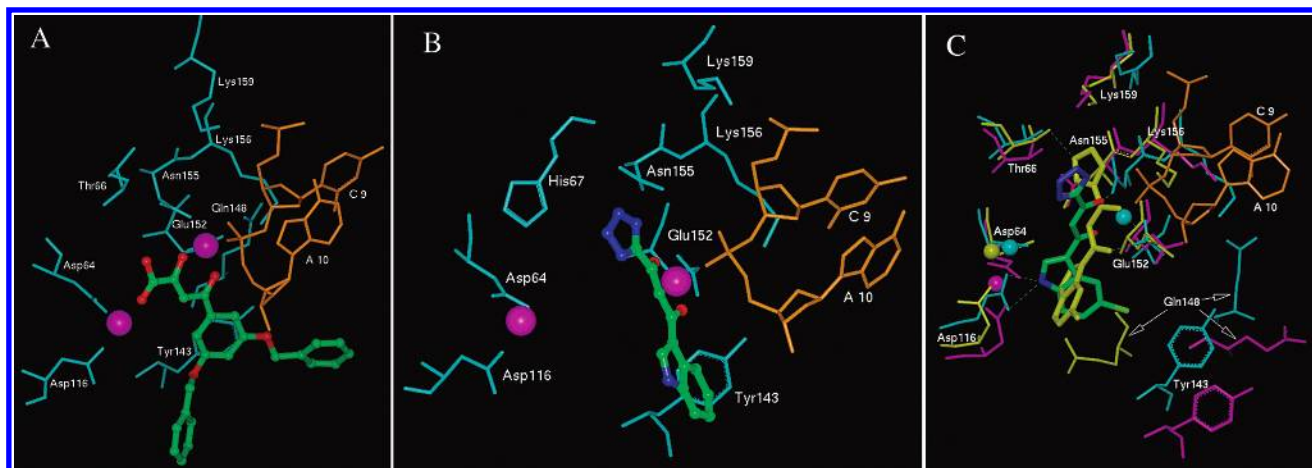


Figure 2. (A) Docking model of L-708,906 in the active site of an IN core-viral DNA complex, prepared by FlexX and refined with MD simulation (500 ps). (B) Docking model of 5CITEP at the active site of an IN core-viral DNA complex, derived by FlexX and refined with MD simulation (300 ps). (C) Comparison of FlexX-derived docking model with the X-ray-determined 5CITEP bound to the free IN core domain (PDB entry: 1QS4). These figures were produced with InsightII 2000.⁴⁰ All balls stand for Mg²⁺ ions. Residues from an IN-DNA complex are colored in light blue; residues from a free dynamics-averaged IN core domain dimer are colored in purple, and residues from the X-ray structure 1QS4 are shown in yellow. The last two nucleotides C–A of viral DNA are shown in orange.

Molecular Modeling. By utilizing the hypothetical model of IN complexed with viral DNA (developed as described above), FlexX-derived docking models were generated for the binding of both L-708,906 (**10e**) and 5CITEP (**13b**) within the active site. Results of these FlexX-derived docking models were quite similar for L-708,906 and 5CITEP (Figure 2). In both cases, coordination of the second Mg²⁺ ion with the common β -diketopropyl moiety differed only slightly. The carboxyl group of L-708,906 bound to the first Mg²⁺ ion in addition to forming a hydrogen-bonding interaction with Asp64 (Figure 2A). The central aromatic ring of L-708,906 exhibited π – π stacking interactions with the side chain of Tyr143, whereas the two benzyl rings showed significant movement during the simulation. Within the duration of the dynamics run, the tetrazole group of 5CITEP failed to reach the Mg²⁺. Instead, it formed hydrogen-bonding interactions with the phosphate group of the terminal adenosine of the viral DNA (Figure 2B). The aromatic ring of 5CITEP formed edge-to-face hydrophobic interactions with the aromatic plane of Tyr143. This model of 5CITEP docked with the IN–DNA complex exhibits geometry which is similar, but not identical, to the published X-ray structure.¹³ In the latter case, the β -diketopropyl functionality also points toward the side chain of Glu152 (Figure 2C). However, the X-ray complex was of IN before 3'-processing had occurred. Following 3'-processing, one would expect that the active site would undergo a change. From our molecular dynamics simulations,²⁷ it was found that the side chains of residues Gln148, Glu152, Asn155, Lys156, and Lys159 altered their conformations and became more ordered after binding to viral DNA and the second Mg²⁺ ion (Figure 2C).

These modeling studies support similar binding modes and mechanisms of action for L-708,906 and 5CITEP. Both inhibitors form strong electrostatic interactions within the active site which was modeled to represent a state following 3'-processing but before strand transfer. For both compounds, it seems reasonable to hypothesize that they may inhibit strand transfer by occupying the active site so as to hinder access of target DNA.

Molecular modeling studies of potential binding to IN complexed with viral DNA indicate that while the carboxyl of L-708,906 can coordinate a second Mg²⁺ ion, the tetrazole group of 5CITEP fails to reach this ion. Instead, some interaction with the terminal phosphate group of the viral DNA was observed during the molecular dynamics simulation.

Conclusions

DKA-based IN inhibitors represent an emerging class with potential relevance for the development of new AIDS therapeutics. Work reported herein examines the structural relationships of two important members of this family, L-708,906 and 5CITEP. Both compounds share a common β -diketopropyl linker yet differ in both their left aryl and right acidic portions. In regard to the right side acidic functionality, it was observed that both tetrazole and carboxyl moieties provide potent inhibition in biochemical ST assays. Only carboxylic acid-bearing agents **4b** and **10e** are antiviral within the concentration range tested. Reasons for the lack of antiviral potency for tetrazole-containing inhibitors are not clear. In regard to the left side functionality, significant diversity is allowed for substituents on the phenyl nucleus of L-708,906 and the indolyl nucleus of 5CITEP. However, in the former case, substituents at the 3-position are favored with the inhibitory potency of 3-mono-benzyloxy analogue slightly exceeding that of parent 3,5-dibenzyloxy L-708,906. Introduction of acidic functionality into the left side aryl portion of compounds having either carboxyl- or tetrazole-based right side acidic functionality results in the enhancement of 3'-P inhibitory potency and a reduction in 3'-P/ST selectivity. As previously indicated, although both L-708,906 and 5CITEP show potent inhibition of IN in biochemical assays, there is a disparity of antiviral activity in cellular assays using HIV-1-infected cells. Neither 5CITEP nor any other of the indole-containing inhibitors exhibit antiviral effects in cellular systems. Alternatively, L-708,906 does provide antiviral protection at low micromolar concentrations. However, several analogues of L-708,906 with varied substituents on the left

side aryl ring while having good inhibitory potencies against IN in biochemical assays, are not antiviral in whole-cell systems. In summary, distinct activity differences appear to exist between inhibitors related to L-708,906 and those related to 5CITEP. Of the analogues prepared in this study, those predicated on L-708,906 appear more promising based on their antiviral activities.

Experimental Section

DNA Oligonucleotides. Oligonucleotides were purchased from IDT Inc. (Coralville, IA) and purified on a 20% (19:1) denaturing polyacrylamide gel using an UV shadow. Purified oligonucleotides were 5'-end labeled by T4-polynucleotide kinase (Gibco BRL/Life Technologies, Rockville, MD) as described previously.³¹

HIV-1 Integrase Inhibition Assay. The in vitro integration assay using recombinant HIV-1 integrase was performed as described previously.³¹ Unless otherwise indicated, the integrase-DNA complexes were preformed by mixing 400 nM HIV-1 integrase with 10 nM 5'-end ³²P-labeled 21-mer double-stranded DNA template for 15 min on ice in a reaction buffer containing 25 mM MOPS, pH 7.2, 25 mM NaCl, 7.5 mM MnCl₂, 0.1 mg/mL BSA, and 14.3 mM β -mercaptoethanol. Inhibitors were then added to the reaction mixtures in a final volume of 10 μ L, and integration reactions were carried out for 1 h at 37 °C. The reactions were quenched by adding 10 μ L of denaturing loading dye. The samples were loaded onto a 20% (19:1) denaturing polyacrylamide gel. The gels were exposed overnight and analyzed using a Molecular Dynamics Phosphorimager (Sunnyvale, CA).

Cells, Transfection, and Infections. The 293T cells (ATCC) were maintained in the presence of Dulbecco's Modified Eagle's Medium (Cellgro), 10% fetal calf serum (HyClone Laboratories), penicillin (50 units/mL; Gibco), and streptomycin (50 μ g/mL; Gibco). The 293T cells were plated at a density of 5×10^6 per 100 mm diameter dish and transfected using a Transfection MBS Mammalian Transfection Kit (Stratagene). Transfected cell supernatants were harvested 48 h after transfection, clarified, and used to infect target cells. The 293T target cells were plated at a density of 1×10^5 per 35 mm diameter dish. The virus-containing medium was diluted 100-fold and was used to infect the 293T target cells for 1 h as previously described.²⁸ The 293T target cells were incubated with medium containing the test compounds for 4 h prior to infection, 1 h during infection, and 24 h postinfection. Compounds exhibiting ST IC₅₀ values ≤ 10 μ M in extracellular HIV integrase assays (Table 1) were selected for evaluation. All compounds were tested initially at 25 μ M concentration, and those agents which achieved $\geq 50\%$ inhibition at 25 μ M (compounds **4b** and **10e**) were examined over a concentration range to determine the IC₅₀ values.

Luciferase Assay. Infected cells were washed with PBS and lysed in 400 μ L of reporter lysis buffer (Promega) 72 h after infection. The samples were subjected to one freeze-thaw cycle, and cell membranes were removed by centrifugation. Luciferase activity was measured following the addition of 100 μ L of substrate (Promega) to 20 μ L of cell lysate using a TD20/20 luminometer (Promega).

Molecular Modeling. The primary docking work was performed on an SGI Octane workstation, running under the IRIX64 version 6.5 operating system, using the molecular modeling software package SYBYL 6.7.1.³² The IN core-viral DNA complex structure was extracted from the structural model we had previously constructed of the complex with the full-length IN with DNA³³ and subjected to further refinement by molecular dynamics (MD) simulation.²⁷ The compounds L-708,906 and 5CITEP were generated in SYBYL and optimized with ab initio calculations at the B3LYP/6-31G* level of theory with the program Gaussian 98.³⁴ L-708,906 and 5CITEP were then docked into the active site of the IN core-viral DNA complex by means of flexible docking, using the program FlexX³⁵ (part of the SYBYL package), after the

necessary changes were made to have the Mg²⁺ ions and DNA be considered as part of the putative active site.

Two of the primary docking models, one for each lead compound, were selected to be refined further by MD simulations. For these models, the programs CHARMM,³⁶ version c27b3, and the CHARMM all-atom force field, version 27,^{37,38} for protein and DNA were used on an SGI Origin 2000 and a Beowulf-type Linux cluster in parallel.³⁹ Force field parameters for the ligands were developed with the software Quanta/CHARMM 2000.⁴⁰ All simulations were performed in explicit aqueous solvent for 500 ps under the following conditions: constant pressure (1 atm) and temperature (310 K), periodic boundary conditions in a water box (sized $96 \times 70 \times 64$ Å³), 12 Å cutoff for van der Waals interactions, and Particle Mesh Ewald summation for electrostatic interactions. Docking models are shown in Figure 1.

Synthesis. General Synthetic Methods. Elemental analyses were obtained from Atlantic Microlab Inc. (Norcross, GA), and fast atom bombardment mass spectra (FABMS) were acquired with a VG Analytical 7070E mass spectrometer under the control of a VG 2035 data system. Where indicated, the FABMS matrixes used were glycerol (Gly) or nitrobenzoic acid (NBA). ¹H-NMR data were obtained on a Bruker 250 MHz or Varian 400 MHz spectrometer. The data are reported in parts per million relative to TMS and referenced to the solvent in which they were run. The solvent was removed by rotary evaporation under reduced pressure, and silica gel chromatography was performed using Merck silica gel 60 with a particle size of 40–63 μ m. Anhydrous solvents were obtained commercially and used without further drying. HPLCs were conducted using a Waters Prep LC4000 system having photodiode array detection. Binary solvent systems were as indicated where A = 0.1% aqueous TFA and B = 0.1% TFA in acetonitrile. Either Vydac C₁₈ Peptide and Protein (10 μ m) or Advantage C₁₈ (5 μ m) was used, in either preparative size (20 mm diameter \times 250 mm long, with a flow rate of 10 mL/min) or semipreparative size (10 mm diameter \times 250 mm long, with a flow rate of 2 mL/min).

Coupling of Aryl Methyl Ketones. Procedure A. To a stirred solution of LHMDS (1.0 M in THF, 3.0 molar equiv) at –78 °C was added dropwise aryl methyl ketone in anhydrous THF, and the resulting mixture was stirred at –20 °C (2 h). The reaction mixture was recooled to –78 °C, and a solution of **11** in THF was added dropwise. The mixture was allowed to warm to room temperature over 1 h and was stirred at room temperature (2 h), and then the reaction was quenched by the addition of saturated aqueous NH₄Cl and subjected to an extractive workup (EtOAc). Evaporation of the solvent provided a residue which was mixed with EtOAc to yield a bright yellow solid. Recrystallization provided the desired product.

Procedure B. To a stirred solution of NaOEt in anhydrous THF at room temperature was added dropwise diethyl oxalate in THF followed by aryl methyl ketone in THF. The resulting orange-yellow mixture was stirred at room temperature (3 h), and then at 50 °C (18 h). The solvent was removed under reduced pressure to yield a yellow residue which was washed with ether and collected by filtration. The collected solid was washed with 1 N aqueous HCl and H₂O, and then dried and recrystallized to provide the desired final diketo product.

Procedure C. To aryl methyl ketone (1 molar equiv) in toluene was added NaH (2.0 molar equiv), and the mixture was stirred (10 min). Then diethyl oxalate (1.5 molar equiv) was added dropwise, and the mixture was stirred at reflux (1 h). The mixture was cooled to room temperature, and a black solid was removed by filtration. The mixture was washed with ether and acidified with 1 N aqueous HCl, and a solid was collected by filtration. This was washed with H₂O and dried to yield the desired product. Alternatively, the aqueous layer resulting after acidification was subjected to an extractive workup (EtOAc) and concentrated under reduced pressure. Purification by silica gel flash chromatography provided the desired product.

Procedure D. To a dry flask at room temperature under argon were added aryl methyl ketone (1 mmol) in toluene (6

mL) and NaH (4 mmol) followed by diethyl oxalate (2 mmol), and the mixture was stirred at 60 °C (3 h). The reaction was quenched by the addition of H₂O, and the mixture was acidified (to pH 6) with 2 N HCl and subjected to an extractive workup (EtOAc). Removal of the solvent and purification by silica gel chromatography provided the desired product.

Ethyl Ester Hydrolysis. Procedure E. The starting material was dissolved in dioxane; 1 N aqueous HCl was added, and the resulting solution was refluxed (4 h). The solvent was removed under reduced pressure, and H₂O was added to provide a yellow precipitate which was collected, washed with water, and dried to provide the final product.

Procedure F. The starting material in EtOH was refluxed (overnight) with KOH (3.8 molar equiv), cooled to room temperature, diluted with H₂O, and adjusted to pH 3 with 3 N aqueous HCl. The resulting precipitate was collected by filtration and dried to provide the desired product.⁴¹

Procedure G. The starting material was dissolved in THF:EtOH (1:1) and stirred (1 h) with 1 N aqueous NaOH (5 molar equiv). The reaction mixture was washed twice with ether, acidified to pH 2 with 2 N aqueous HCl, and subjected to an exhaustive extractive workup (EtOAc) to provide the desired product following purification.

Procedure H. A solution of ester (0.3 mmol) in dioxane (3 mL) was stirred with 1 N NaOH (3 mL, 1 h), and then acidified to pH 4–5 with 2 N aqueous HCl and taken to dryness. Pure product was produced following preparative HPLC purification.

Indole Acylation. Procedure I. To a solution of ammonium chloride (4 molar equiv) suspended in ethylene dichloride was added dropwise via syringe acetic anhydride (2 molar equiv) at room temperature, and the mixture was stirred at room temperature (15 min). After the mixture had been stirred for 15 min, indicated indoles (1 molar equiv) in ethylene dichloride were added dropwise. As the mixture was stirred at room temperature (2 h), AlCl₃ (2 molar equiv) was added, changing the heterogeneous mixtures to homogeneous mixtures. Acetic anhydride (1 mol equiv) was added, and the mixture was stirred (30 min); the mixtures were then poured into crushed ice and subjected to extractive workups (EtOAc). The concentration provided residues which were crystallized from EtOAc.

Removal of Pmb Functionality. Procedure J. A mixture of Pmb-containing compound, TFA, and ethylenedithiol/H₂O (1:1) was stirred at room temperature (20 h), and then volatiles were removed under reduced pressure. The residue was triturated with ether, and the resulting yellow solid was resuspended in ether, washed with H₂O and EtOAc, and dried to provide the deprotected product.

N-(3-Acetylphenyl)benzamide (2c). To a mixture of 3'-aminoacetophenone (406 mg, 3 mmol) in pyridine (10 mL) was added phenylcarbonyl benzoate (814 mg, 3.6 mmol), and the mixture was stirred at room temperature overnight. After the reaction was completed, the mixture was poured into ice cold water (20 mL) and extracted with diethyl ether (20 mL × 3). The organic layers were combined and dried over Na₂SO₄. After removal of the solvent, the residue was chromatographed (3:1 ratio of hexanes:EtOAc) to provide **2c** as a solid (84% yield): mp 97–99 °C; H-NMR (CDCl₃, δ) 8.28 (1H, s), 8.14 (1H, t, *J* = 2 Hz), 8.06 (1H, m), 7.87 (2H, m), 7.67 (1H, dt, *J* = 8, 1 Hz), 7.56–7.40 (4H, m), 2.55 (3H, s); FABMS (+VE) *m/z* 240 (M + H)⁺.

Ethyl 2-Hydroxy-4-oxo-4-[3-(phenylcarbonylamino)-phenyl]but-2-enoate (3c). The compound **2c** was treated according to general procedure D to provide **3c** as a solid (99% yield): mp 100–101 °C; H-NMR (CDCl₃, δ) 8.10 (1H, s), 8.07–8.04 (2H, m), 7.86 (2H, d, *J* = 7 Hz), 7.74 (1H, d, *J* = 8 Hz), 7.57–7.42 (4H, m), 7.04 (1H, s), 4.37 (2H, q, *J* = 8 Hz), 1.39 (3H, t, *J* = 8 Hz); FABMS (+VE) *m/z* 340 (M + H)⁺. Anal. (C₁₉H₁₇NO₃) C, H, N.

Ethyl 2-Hydroxy-4-oxo-(4-phenoxyphenyl)but-2-enoate (3d). Compound **2d** was treated according to general procedure D to provide **3d** as an oil (83% yield): H-NMR (CDCl₃, δ) 8.05–7.97 (2H, m), 7.44–7.40 (2H, t, *J* = 7.7 Hz), 7.24–

7.21 (2H, m), 7.11–7.02 (4H, m), 4.40 (2H, q), 1.42 (3H, t); FABMS (+VE) *m/z* 313 (M + H)⁺.

4-(3-Bromophenyl)-2-hydroxy-4-oxobut-2-enoic Acid (4a). Treatment of **3a** according to general procedure H provided **4a** as a solid (91% yield): mp 149–150 °C; H-NMR (DMSO-*d*₆, δ) 8.18 (1H, t, *J* = 2 Hz), 8.06 (1H, d, *J* = 8 Hz), 7.87 (1H, d, *J* = 8 Hz), 7.52 (1H, t, *J* = 8 Hz), 7.09 (1H, s); FABMS (–VE) *m/z* 269 (M – H)[–]. Anal. (C₁₀H₇BrO₄·0.93H₂O) C, H.

2-Hydroxy-4-oxo-4-[3-(phenylmethoxy)phenyl]but-2-enoic Acid (4b). Treatment of **3b** according to general procedure H provided **4b** as a solid (30% yield): mp 148–149 °C; H-NMR (DMSO-*d*₆, δ) 7.51–7.65 (1H, d, *J* = 8 Hz), 7.62 (1H, d, *J* = 2 Hz), 7.51–7.32 (7H, m), 7.06 (1H, s); FABMS (–VE) *m/z* 297 (M – H)[–]. Anal. (C₁₇H₁₄O₅) C, H.

2-Hydroxy-4-oxo-4-[3-(phenylcarbonylamino)phenyl]but-2-enoic Acid (4c). Treatment of **3c** according to general procedure H provided **4c** as a solid (55% yield): mp 184–185 °C; H-NMR (DMSO-*d*₆, δ) 10.48 (1H, s), 8.48 (1H, s), 8.17 (1H, d, *J* = 9 Hz), 7.99 (2H, d, *J* = 7 Hz), 7.80 (1H, d, *J* = 8 Hz), 7.62–7.53 (4H, m), 7.06 (1H, s); FABMS (–VE) *m/z* 310 (M – H)[–]. Anal. (C₁₇H₁₃NO₅·0.7H₂O) C, H, N.

2-Hydroxy-4-oxo-(4-phenoxyphenyl)but-2-enoic Acid (4d). Treatment of **3d** according to general procedure H provided **4d** as a solid (61% yield): mp 179–180 °C; H-NMR (DMSO-*d*₆, δ) 8.09 (2H, d, *J* = 8.8 Hz), 7.48 (2H, t, *J* = 8.8 Hz), 7.27 (1H, t, *J* = 7 Hz), 7.16 (2H, d, *J* = 8 Hz), 7.08–7.03 (3H, m); FABMS (–VE) *m/z* 283 (M – H)[–]. Anal. (C₁₆H₁₂O₅·0.22H₂O) C, H.

2-Hydroxy-4-oxo-4-phenylbut-2-enoic Acid (4e). Acetophenone was treated according to general procedure C to provide **4e** which was recrystallized from ether/hexane to provide **4e** as a yellow solid⁴² (75% yield): mp 155–158 °C; H-NMR (CDCl₃, δ) 7.15 (1H, s), 7.53 (2H, t, *J* = 7.3 Hz), 7.65 (1H, t, *J* = 7.3 Hz), 8.00 (2H, d, *J* = 7.1 Hz); FABMS (+VE) *m/z* 191 (M + H)⁺.

2,4-Diacetylquinoline (5c). Compound **5c** was obtained as a white solid according to literature procedures:⁴³ mp 66–68 °C (lit.⁴⁴ 69 °C); H-NMR (CDCl₃, δ) 2.80 (3H, s), 2.90 (3H, s), 7.72–7.88 (2H, m), 8.27 (1H, dd, *J* = 7.3, 1.2 Hz), 8.39 (1H, s), 8.57 (1H, dd, *J* = 6.8, 0.5 Hz); FABMS (+VE) *m/z* 214 (M + H)⁺.

Ethyl 4-[3-(3-Ethoxycarbonyl-3-hydroxyprop-2-enoyl)-phenyl]-2-hydroxy-4-oxobut-2-enoate (6a). In a modification of general procedure B, diketone **5a** (0.50 g, 3.08 mmol) was coupled with diethyl oxalate (1.80 g, 12.3 mmol) using NaOEt (0.85 g, 12.5 mmol) in THF (25 mL) to provide a yellow residue. The residue was suspended in 1 N aqueous HCl, filtered, washed with H₂O, and dried to provide the desired product **6a** as a yellow solid (0.89 g, 80% yield) after crystallization (EtOAc): mp 93–95 °C; H-NMR (DMSO-*d*₆, δ) 1.37 (6H, t, *J* = 7.1 Hz), 4.39 (4H, q, *J* = 7.1 Hz), 7.21 (2H, s), 7.81 (1H, t, *J* = 7.8 Hz), 8.38 (2H, d, *J* = 7.6 Hz), 8.59 (1H, s); FABMS (+VE) *m/z* 363 (M + H)⁺. Anal. (C₁₈H₁₈O₈·0.22CH₃·CO₂C₂H₅) C, H.

Ethyl 4-[4-(3-Ethoxycarbonyl-3-hydroxyprop-2-enoyl)-phenyl]-2-hydroxy-4-oxobut-2-enoate (6b). The treatment of diketone **5b** (1.0 g, 6.17 mmol) as described above for the preparation of **6a** provided the desired product **6b** as a shiny yellow solid (1.83 g, 82% yield) after crystallization (EtOAc): mp 113–115 °C (lit.⁴⁵ mp 160 °C); H-NMR (DMSO-*d*₆, δ) 1.37 (6H, t, *J* = 7.1 Hz), 4.37 (4H, q, *J* = 7.1 Hz), 7.19 (2H, s), 8.25 (4H, s); FABMS (+VE) *m/z* 363 (M + H)⁺. Anal. (C₁₈H₁₈O₈) C, H.

Ethyl 4-[4-(3-Ethoxycarbonyl-3-hydroxyprop-2-enoyl)-2-quinolyl]-2-hydroxy-4-oxobut-2-enoate (6c). Treatment of diketone **5c** as described above for the preparation of **6a** provided the desired product **6c** as a solid (77% yield) after crystallization (EtOAc): mp 148–150 °C; H-NMR (DMSO-*d*₆, δ) 1.22 (3H, t, *J* = 7.3 Hz), 1.33 (3H, t, *J* = 7.3 Hz), 4.11 (2H, q, *J* = 6.6 Hz), 4.32 (2H, q, *J* = 6.6 Hz), 7.48 (1H, s), 7.73 (1H, t, *J* = 7.3 Hz), 7.88 (1H, t, *J* = 7.3 Hz), 8.05 (1H, s), 8.21 (1H, d, *J* = 8.8 Hz), 8.32 (1H, d, *J* = 8.1 Hz); FABMS (+VE) *m/z* 414 (M + H)⁺.

4-[3-(3-Carboxy-3-hydroxyprop-2-enoyl)phenyl]-2-hydroxy-4-oxobut-2-enoic Acid (7a). Treatment of diester **6a** according to general procedure F gave a yellow solid. Recrystallization (AcOH) provided diacid **7a** as beige solid (75% yield): mp >250 °C; H-NMR (DMSO- d_6 , δ) 7.01 (2H, s), 7.76 (1H, t, J = 8.1 Hz), 8.31 (2H, d, J = 7.6 Hz), 8.56 (1H, s); FABMS ($^{-}$ VE) m/z 305 (M - H) $^{-}$. HRMS calcd for C₁₄H₉O₈: 305.0297. Found: 305.0303.

4-[4-(3-Carboxy-3-hydroxyprop-2-enoyl)phenyl]-2-hydroxy-4-oxobut-2-enoic Acid (7b). Treatment of diester **6b** as described in general procedure F and crystallization of the product from EtOAc provided **7b** as a yellow solid (78% yield): mp 249–250 °C; H-NMR (DMSO- d_6 , δ) 7.17 (2H, s), 8.23 (4H, s); FABMS ($^{-}$ VE) m/z 306 (M) $^{-}$.

4-[4-(3-Carboxy-3-hydroxyprop-2-enoyl)-2-quinoly]-2-hydroxy-4-oxobut-2-enoic Acid (7c). Treatment of diester **6c** as described in general procedure G provided a brown solid in 65% yield by HPLC: H-NMR (DMSO- d_6 , δ) 6.69 (2H, s), 7.85 (1H, t, J = 8.1 Hz), 7.97 (1H, t, J = 6.6 Hz), 8.13 (1H, s), 8.29 (2H, t, J = 8.1 Hz); FABMS ($^{-}$ VE) m/z 356 (M - H) $^{-}$. Anal. (C₁₇H₁₁NO₈·0.84H₂O) C, H, N.

3-Acetyl-5-chloroindole (8b). Compound **8b** was prepared according to general procedure I and was obtained as a white solid in 75% yield: H-NMR (DMSO- d_6 , δ) 2.45 (3H, s), 7.22 (1H, dd, J = 8.1, 2.2 Hz), 7.49 (1H, d, J = 8.8 Hz), 8.14 (1H, s), 8.38 (1H, d, J = 2.9 Hz), 12.10 (1H, brs); FABMS ($^{+}$ VE) m/z 194 (M + H) $^{+}$.

4-Acetylquinoline (8c). Compound **8c** was obtained as a white solid according to literature procedures:⁴³ mp 50–51 °C; H-NMR (CDCl₃, δ) 2.83 (3H, s), 7.61–7.84 (2H, m), 7.87 (1H, d, J = 8.1 Hz), 8.10–8.31 (3H, m); FABMS ($^{+}$ VE) m/z 172 (M + H) $^{+}$.

3-Acetyl-5-fluoroindole (8f). Compound **8f** was prepared according to general procedure I and was obtained as a white solid in 73% yield: mp 200–201 °C (lit.⁴⁶ 200–201.5 °C); H-NMR (DMSO- d_6 , δ) 2.48 (3H, s), 7.11 (1H, td, J = 6.1, 2.4 Hz), 7.52 (1H, dd, J = 4.6, 4.2 Hz), 7.86 (1H, dd, J = 10, 2.2 Hz), 8.42 (1H, d, J = 2.9 Hz), 12.06 (1H, brs); FABMS ($^{+}$ VE) m/z 178 (M + H) $^{+}$.

Benzyl 3-Acetylindole-5-carboxylate (8g). A mixture of indole-5-carboxylic acid (0.20 g, 1.24 mmol), benzyl bromide (0.89 mL, 7.45 mmol), and NaHCO₃ (0.63 g, 7.45 mmol) in DMF (5 mL) was stirred at room temperature (3 days). The mixture was poured into H₂O and subjected to an extractive workup (EtOAc), and the residue crystallized in EtOAc to provide benzyl indole-5-carboxylate as a colorless solid (0.28 g, 90% yield):⁴⁷ mp 128–130 °C (lit.⁴⁸ 127–129 °C); H-NMR (CDCl₃, δ) 5.49 (2H, s), 6.73 (1H, d, J = 2.2 Hz), 7.33–7.60 (6H, m), 8.05 (1H, dd, J = 7.1, 1.5 Hz), 8.57 (2H, s). Acylation as indicated in general procedure I provided **8g** as a colorless solid in 65% yield: mp 217–219 °C; H-NMR (DMSO- d_6 , δ) 2.55 (3H, s), 5.36 (2H, s), 7.30–7.60 (6H, m), 7.86 (1H, dd, J = 6.6, 2.2 Hz), 8.45 (1H, s), 8.89 (1H, d, J = 1.5 Hz), 12.31 (1H, brs); FABMS ($^{+}$ VE, NBA) m/z 294 (M + H) $^{+}$. Anal. (C₁₈H₁₅NO₃·0.002H₂O) C, H, N.

Ethyl 4-(Indol-3-yl)-2-hydroxy-4-oxobut-2-enoate (9a). Treatment of 3-acetyl indole (**8a**) as indicated in general procedure B with recrystallization from MeOH/hexane gave **9a** as a yellow solid (80% yield): mp >300 °C; H-NMR (DMSO- d_6 , δ) 1.35 (3H, t, J = 7.1 Hz), 4.31 (2H, q, J = 7.1 Hz), 6.97 (1H, s), 7.28 (2H, t, J = 3.6 Hz), 7.53 (1H, d, J = 6.4 Hz), 8.28 (1H, d, J = 7.1 Hz), 8.67 (1H, s); FABMS ($^{+}$ VE) m/z 260 (M + H) $^{+}$. Anal. (C₁₄H₁₃NO₄) C, H, N.

Ethyl 4-(5-Chloroindol-3-yl)-2-hydroxy-4-oxobut-2-enoate (9b). Treatment of 3-acetyl-5-chloroindole as indicated in general procedure B with recrystallization of the product from dioxane gave **9b** as a yellow solid (82% yield): mp 219–225 °C; H-NMR (DMSO- d_6 , δ) 1.36 (3H, t, J = 7.1 Hz), 4.35 (2H, q, J = 7.1 Hz), 7.08 (1H, s), 7.35 (1H, d, J = 8.5 Hz), 7.75 (1H, d, J = 8.6 Hz), 8.25 (1H, s), 8.87 (1H, d, J = 1.2 Hz), 12.67 (1H, brs); FABMS ($^{+}$ VE) m/z 294 (M + H) $^{+}$.

Ethyl 4-(Quinol-4-yl)-2-hydroxy-4-oxobut-2-enoate (9c). Treatment of 4-acetylquinoline according to general procedure B gave **9c** as a brown solid (86% yield): mp 145–150 °C;

H-NMR (DMSO- d_6 , δ) 1.33 (3H, t, J = 6.8 Hz), 4.27 (2H, q, J = 7.1 Hz), 7.22 (1H, s), 7.73 (1H, t, J = 8.5 Hz), 7.88 (1H, t, J = 8.5 Hz), 8.08 (1H, d, J = 7.6 Hz), 8.18 (2H, d, J = 8.1 Hz), 8.53 (1H, d, J = 7.6 Hz); FABMS ($^{+}$ VE) m/z 272 (M + H) $^{+}$.

Ethyl 4-(2-Ferrocenyl)-2-hydroxy-4-oxobut-2-enoate (9d). Treatment of acetylferrocene as described in general procedure C and purification of the product by silica gel flash chromatography (20:80 ratio of EtOAc:hexane) gave pure **9d** as a violet solid (60% yield): mp 66–69 °C; H-NMR (CDCl₃, δ) 1.42 (3H, t, J = 7.1 Hz), 4.26 (5H, s), 4.39 (2H, q, J = 7.1 Hz), 4.68 (2H, s), 4.92 (2H, s), 6.56 (1H, s); FABMS ($^{+}$ VE) m/z 328 (M + H) $^{+}$.

Ethyl 4-[(3,5-Dibenzyloxy)phen-1-yl]-2-hydroxy-4-oxobut-2-enoate (9e). Treatment of 3,5-dibenzyloxyacetophenone (**8e**) as described in general procedure B and crystallization of the product from EtOAc/hexane gave **9e** as a bright yellow solid: mp 77–78 °C; H-NMR (CDCl₃, δ) 1.51 (3H, t, J = 7.1 Hz), 4.49 (2H, q, J = 7.1 Hz), 5.18 (4H, s), 6.95 (1H, s), 7.11 (1H, s), 7.33 (2H, s), 7.35–7.59 (10H, m); FABMS ($^{+}$ VE) m/z 433 (M + H) $^{+}$. Anal. (C₂₆H₂₄O₆·0.026CH₃CO₂C₂H₅) C, H.

4-(Indol-3-yl)-2-hydroxy-4-oxobut-2-enoic Acid (10a). Treatment of ester **9a** as described in general procedure E and crystallization from EtOAc provided **10a** as a yellow solid (56% yield):²⁵ mp 202–210 °C; H-NMR (DMSO- d_6 , δ) 7.06 (1H, s), 7.30 (2H, t, J = 3.6 Hz), 7.53 (1H, s), 8.27 (1H, s), 8.75 (1H, d, J = 2.7 Hz), 12.44 (1H, s); FABMS ($^{-}$ VE) m/z 230 (M - H) $^{-}$.

4-(5-Chloroindol-3-yl)-2-hydroxy-4-oxobut-2-enoic Acid (10b). Treatment of ester **9b** as described in general procedure E provided **10b** as a brown solid (65% yield): mp 220–225 °C (lit.²⁴ 220–225 °C); H-NMR (DMSO- d_6 , δ) 7.06 (1H, s), 7.29 (1H, dd, J = 8.7, 2.4 Hz), 7.53 (1H, d, J = 8.7 Hz), 8.21 (1H, d, J = 2.4 Hz), 8.77 (1H, d, J = 3.6 Hz), 12.5 (1H, brm).

2-Hydroxy-4-oxo-4-(quinolin-4-yl)but-2-enoic Acid (10c). Treatment of ester **9c** as described in general procedure G and purification by HPLC provided **10c** as a yellow solid (75% yield): H-NMR (DMSO- d_6 , δ) 7.74 (1H, t, J = 8.1 Hz), 7.86 (1H, t, J = 8.8 Hz), 8.08 (1H, d, J = 9.5 Hz), 8.14 (2H, t, J = 8.8 Hz), 8.55 (1H, d, J = 8.8 Hz); FABMS ($^{-}$ VE) m/z 242 (M - H) $^{-}$.

4-(2-Ferrocenyl)-2-hydroxy-4-oxobut-2-enoic Acid (10d). Treatment of ester **9d** as described in general procedure G and purification by silica gel flash chromatography (90:10 ratio of CHCl₃:MeOH) provided **10d** as a violet solid (60% yield): mp 160–163 °C; H-NMR (CDCl₃, δ) 4.23 (5H, s), 4.69 (2H, s), 4.92 (2H, s), 7.27 (1H, s); FABMS ($^{-}$ VE) m/z 299 (M - H) $^{-}$. HR-FABMS calcd for C₁₄H₁₁FeO₄ (M - H): 299.00067. Found: 299.00158.

4-[(3,5-Dibenzyloxy)phen-1-yl]-2-hydroxy-4-oxobut-2-enoic Acid (10e). Treatment of ester **9e** as described in general procedure E and crystallization from EtOAc provided **10e** as a yellow solid (75% yield): mp 170–172 °C; H-NMR (DMSO- d_6 , δ) 5.15 (4H, s), 6.95 (1H, t, J = 2.3 Hz), 7.03 (1H, s), 7.21 (2H, d, J = 2.3 Hz), 7.35–7.61 (10H, m); FABMS ($^{-}$ VE) m/z 403 (M - H) $^{-}$. Anal. (C₂₄H₂₀O₆·0.15CH₃CO₂C₂H₅) C, H.

Ethyl 1-(4-Methoxybenzyl)tetrazole-5-carboxylate (11). By using literature procedures,²⁶ compound **11** was obtained as a white solid in 58% yield: mp 51–53 °C (lit.²⁶ 50–52 °C); H-NMR (CDCl₃, δ) 1.39 (3H, t, J = 7.1 Hz), 3.85 (3H, s), 4.47 (2H, q, J = 7.1 Hz), 5.80 (2H, s), 6.81 (2H, d, J = 8.8 Hz), 7.42 (2H, d, J = 8.8 Hz).

1-(Indol-3-yl)-3-hydroxy-3-[1-(4-methoxybenzyl)tetrazol-5-yl]propenone (12a). Coupling of **8a** with **11** as indicated in general procedure A and crystallization from EtOAc provided **12a** as a yellow solid (88% yield): mp 210–215 °C; H-NMR (DMSO- d_6 , δ) 3.69 (3H, s), 6.88 (2H, d, J = 10.3 Hz), 7.20 (1H, s), 7.20–7.27 (2H, m), 7.28 (2H, d, J = 10.5 Hz), 7.45–7.51 (1H, m), 8.09–8.15 (1H, m), 8.64 (1H, d, J = 5.2 Hz); FABMS ($^{+}$ VE) m/z 376 (M + H) $^{+}$.

1-(5-Chloroindol-3-yl)-3-hydroxy-3-[1-(4-methoxybenzyl)tetrazol-5-yl]propenone (12b). Coupling of **8b** with **11** as indicated in general procedure A and crystallization from EtOAc to provide **12b** as a yellow solid (84% yield): mp 200–205 °C; H-NMR (DMSO- d_6 , δ) 3.72 (3H, s), 5.94 (2H, s), 6.96 (2H, d, J = 7.3 Hz), 7.28 (1H, s), 7.36 (3H, d, J = 8.8 Hz), 7.53

(1H, d, $J = 8.1$ Hz), 8.25 (1H, s), 8.58 (1H, s), 12.38 (1H, brs); FABMS (+VE) m/z 410 (M + H)⁺. HR-FABMS calcd for C₂₀H₁₅ClN₅O₃ (M - H): 408.0863. Found: 408.0878.

1-(5-Fluorindol-3-yl)-3-hydroxy-3-[1-(4-methoxybenzyl)tetrazol-5-yl]propenone (12f). Coupling of **8f** with **11** as indicated in general procedure A provided **12f** as a yellow solid (60% yield): mp 212–215 °C; H-NMR (DMSO-*d*₆, δ) 3.76 (3H, s), 5.97 (2H, s), 6.97 (2H, d, $J = 8.3$ Hz), 7.19 (1H, t, $J = 9.5$ Hz), 7.28 (1H, s), 7.38 (2H, d, $J = 8.5$ Hz), 7.58 (1H, dd, $J = 3.4, 4.4$ Hz), 7.90 (1H, d, $J = 8.8$ Hz), 8.89 (1H, s), 12.71 (1H, brs); FABMS (+VE) m/z 394 (M + H)⁺. HR-FABMS calcd for C₂₀H₁₅FN₅O₃ (M - H): 392.1159. Found: 392.1143.

1-[(5-Benzyloxy)carbonyl]indol-3-yl)-3-hydroxy-3-[1-(4-methoxybenzyl)tetrazol-5-yl]propenone (12g). Coupling of **8g** with **11** as indicated in general procedure A and crystallization from EtOAc provided **12g** as a yellow solid (75% yield): mp 195–198 °C; H-NMR (DMSO-*d*₆, δ) 3.47 (3H, s, $J = 3$ Hz), 5.32 (2H, s), 5.82 (2H, s), 6.40 (2H, d, $J = 8.5$ Hz), 6.91 (1H, s), 7.28–7.56 (8H, m), 7.87 (1H, dd, $J = 6.8, 1.7$ Hz), 8.39 (1H, s), 9.38 (1H, s), 12.16 (1H, brs); FABMS (+VE, NBA) m/z 510 (M + H)⁺. HR-FABMS calcd for C₂₈H₂₂N₅O₅ (M - H): 508.1621. Found: 508.1627.

1-(Indol-3-yl)-3-hydroxy-3-(1H-tetrazol-5-yl)propenone (13a). Treatment of **12a** as described in general procedure J provided a yellow solid which was recrystallized from DMF to provide **13a** as a yellow solid (75% yield): mp 235–240 °C; H-NMR (DMSO-*d*₆, δ) 7.25 (1H, s), 7.26–7.31 (2H, m), 7.51–7.55 (1H, m), 8.22 (1H, dd, $J = 5.9, 2.9$ Hz), 8.76 (1H, d, $J = 3.7$ Hz), 12.45 (1H, s); CIMS (NH₃) m/z 273 (M + NH₄)⁺. Anal. (C₁₂H₉N₅O₂·0.86C₃H₇NO) C, H, N.

1-(5-Chloroindol-3-yl)-3-hydroxy-3-(1H-tetrazol-5-yl)propenone (13b). Treatment of **12b** as described in general procedure J provided **13b** as a yellow solid (70% yield): mp 250 °C; H-NMR (DMSO-*d*₆, δ) 7.26 (1H, s), 7.32 (1H, dd, $J = 8.7, 2.1$ Hz), 7.56 (1H, d, $J = 8.7$ Hz), 8.21 (1H, d, $J = 2.1$ Hz), 8.84 (1H, d, $J = 3.3$ Hz), 12.6 (1H, brs); FABMS (−VE) m/z 288 (M - H)⁺.

1-(5-Fluorindol-3-yl)-3-hydroxy-3-(1H-tetrazol-5-yl)propenone (13f). Treatment of **12f** as described in general procedure J provided **13f** as a yellow solid (86% yield): mp 260 °C dec; H-NMR (DMSO-*d*₆, δ) 7.15–7.31 (2H, m), 7.55–7.58 (1H, m), 7.89–7.99 (1H, m), 8.89 (1H, t, $J = 3.2$ Hz), 12.63 (1H, brs); FABMS (+VE) m/z 274 (M + H)⁺.

1-(5-Carboxyindol-3-yl)-3-hydroxy-3-(1H-tetrazol-5-yl)propenone (13g). A solution of **12g** (0.05 g, 0.098 mmol) in THF (2 mL) with Pd·C (100 mg) was stirred at room temperature under H₂ supplied by a balloon (4 h). The mixture was filtered through Celite, and the filter pad was washed thoroughly with THF. The combined organic layer was dried, concentrated under reduced pressure, and then treated as indicated in general procedure J to provide the desired product **13g** as a yellow solid (10 mg, 34% yield): H-NMR (DMSO-*d*₆, δ) 7.28 (1H, s), 7.62 (1H, dd, $J = 8.3, 0.98$ Hz), 7.92 (1H, d, $J = 12.5$ Hz), 8.85 (1H, s), 8.95 (1H, s), 12.68 (1H, brs); FABMS (−VE, NBA) m/z 298 (M - H)[−]. Anal. (C₁₃H₉N₅O₄) C, H, N.

Ethyl 1-(3,5-Dimethoxybenzyl)tetrazole-5-carboxylate (14). A mixture of 3,5-dimethoxybenzyl bromide (1.0 g, 4.33 mmol) and sodium azide (0.338 g, 5.19 mmol) in 70% aqueous EtOH (5 mL) was stirred at 58 °C (overnight). The mixture was cooled to room temperature, diluted with H₂O, and subjected to an extractive workup (CHCl₃). Concentration and purification by silica gel flash chromatography (95:5 ratio of hexane:EtOAc) provided the intermediate 3,5-dimethoxybenzyl azide as a colorless oil (0.68 g, 81% yield): H-NMR (CDCl₃, δ) 3.80 (6H, s), 4.27 (2H, s), 6.43 (1H, t, $J = 2.2$ Hz), 6.46 (2H, d, $J = 2.2$ Hz). Treatment of 3,5-dimethoxybenzyl azide in a manner similar to that used to prepare compound **11** provided **14** as a white solid in 70% yield: mp 95–97 °C; H-NMR (CDCl₃, δ) 1.41 (3H, t, $J = 7.1$ Hz), 3.72 (6H, s), 4.47 (2H, q, $J = 7.1$ Hz), 5.8 (2H, s), 6.37 (1H, t, $J = 2.2$ Hz), 6.44 (2H, d, $J = 2.2$ Hz); FABMS (+VE) m/z 293 (M + H)⁺. Anal. (C₁₃H₁₆N₄O₄) C, H, N.

1-(Indol-3-yl)-3-hydroxy-3-[1-(3,5-dimethoxybenzyl)tetrazol-5-yl]propenone (15a). Coupling of **8a** with **14** as

indicated in general procedure A and crystallization from EtOAc provided **15a** as a yellow solid (85% yield): mp 217–218 °C; H-NMR (DMSO-*d*₆, δ) 3.75 (6H, s), 5.98 (2H, s), 6.48–6.55 (3H, m), 7.27–7.38 (3H, m), 7.53–7.61 (1H, m), 8.18–8.25 (1H, m), 8.82 (1H, s), 12.6 (1H, s); FAB-MS (+VE) m/z 406 (M + H)⁺. HR-FABMS calcd for C₂₁H₁₈N₅O₄ (M - H): 404.1359. Found: 404.1367.

1-[(3,5-Dibenzyloxy)phen-1-yl]-3-hydroxy-3-[1-(4-methoxybenzyl)tetrazol-5-yl]propenone (16b). Coupling of **8e** with **11** as indicated in general procedure A provided **16b** as a yellow solid (60% yield): mp 118–120 °C; H-NMR (CDCl₃, δ) 3.78 (3H, s), 5.09 (4H, s), 5.94 (2H, s), 6.85 (1H, s), 6.89 (1H, s), 7.23 (2H, s), 7.31–7.49 (10H, m); FABMS (+VE) m/z 549 (M + H)⁺.

References

- (1) A preliminary account of this information has been presented in: Burke, T. R., Jr.; Pais, C. G.; Zhang, X.; Marchand, C.; Neamati, N.; Pommier, Y.; Svarovskaia, E. S.; Pathak, V. K. Structure–activity investigation of 3-aryl-1,3-diketo containing compounds as HIV-1 integrase inhibitors. Second HIV DRP Symposium: Antiviral Drug Resistance, Chantilly, VA, 2001.
- (2) Palella, F. J., Jr.; Delaney, K. M.; Moorman, A. C.; Loveless, M. O.; Fuhrer, J.; Satten, G. A.; Aschman, D. J.; Holmberg, S. D. Declining morbidity and mortality among patients with advanced human immunodeficiency virus infection. HIV Outpatient Study Investigators. *N. Engl. J. Med.* **1998**, *338*, 853–860.
- (3) Richman, D. D. HIV chemotherapy. *Nature* **2001**, *410*, 995–1001.
- (4) LaFemina, R. L.; Schneider, C. L.; Robbins, H. L.; Callahan, P. L.; LeGrow, K.; Roth, E.; Schleif, W. A.; Emini, E. A. Requirement of active human immunodeficiency virus type 1 integrase for productive infection of human T-lymphoid cells. *J. Virol.* **1992**, *66*, 7414–7419.
- (5) Pommier, Y.; Neamati, N. Inhibitors of human immunodeficiency virus integrase. *Adv. Virus Res.* **1999**, *52*, 427–458.
- (6) Farnet, C. M.; Wang, B. B.; Lipford, J. R.; Bushman, F. D. Differential inhibition of HIV-1 preintegration complexes and purified integrase protein by small molecules. *Proc. Natl. Acad. Sci. U.S.A.* **1996**, *93*, 9742–9747.
- (7) Pommier, Y.; Marchand, C.; Neamati, N. Retroviral integrase inhibitors year 2000: update and perspectives. *Antiviral Res.* **2000**, *47*, 139–148.
- (8) Fujishita, T.; Yoshinaga, T.; Sato, A. (Shionogi & Co., Ltd.). Preparation of aromatic heterocycle compounds having HIV integrase inhibiting activities. PCT Int. Appl. WO-00039086, 2000; pp 554.
- (9) Uenaka, M.; Kawata, K.; Nagai, M.; Endoh, T. (Shionogi & Co., Ltd.). Novel processes for the preparation of substituted propenone derivatives. PCT Int. Appl. WO-00075122, 2000; pp 97.
- (10) Selnick, H. G.; Hazuda, D. J.; Egbertson, M.; Guare, J. P., Jr.; Wai, J. S.; Young, S. D.; Clark, D. L.; Medina, J. C. (Merck and Co., Inc.). Preparation of nitrogen-containing 4-heteroaryl-2,4-dioxobutyric acids useful as HIV integrase inhibitors. PCT Int. Appl. WO-09962513, 1999; pp 287.
- (11) Young, S. D.; Egbertson, M.; Payne, L. S.; Wai, J. S.; Fisher, T. E.; Guare, J. P., Jr.; Embrey, M. W.; Tran, L.; Zhuang, L.; Vacca, J. P.; Langford, M.; Melamed, J.; Clark, D. L.; Medina, J. C.; Jaen, J. (Merck and Co., Inc.). Preparation of aromatic and heteroaromatic 4-aryl-2,4-dioxobutyric acid derivatives useful as HIV integrase inhibitors. PCT Int. Appl. WO-9962520, 1999; pp 319.
- (12) Payne, L. S.; Tran, L. O.; Zhuang, L. H.; Young, S. D.; Egbertson, M. S.; Wai, J. S.; Embrey, M. W.; Fisher, T. E.; Guare, J. P.; Langford, H. M.; Melamed, J. Y.; Clark, D. L. Preparation of 1,3-diaryl-1,3-propanediones as HIV integrase inhibitors. PCT Int. Appl. WO-0100578 (Merck & Co., Inc.; Tularik, Inc.). USA, 2001; pp 236.
- (13) Goldgur, Y.; Craigie, R.; Cohen, G. H.; Fujiwara, T.; Yoshinaga, T.; Fujishita, T.; Sugimoto, H.; Endo, T.; Murai, H.; Davies, D. R. Structure of the HIV-1 integrase catalytic domain complexed with an inhibitor: A platform for antiviral drug design. *Proc. Natl. Acad. Sci. U.S.A.* **1999**, *96*, 13040–13043.
- (14) Espeseth, A. S.; Felock, P.; Wolfe, A.; Witmer, M.; Grobler, J.; Anthony, N.; Egbertson, M.; Melamed, J. Y.; Young, S.; Hamill, T.; Cole, J. L.; Hazuda, D. J. HIV-1 integrase inhibitors that compete with the target DNA substrate define a unique strand transfer conformation for integrase. *Proc. Natl. Acad. Sci. U.S.A.* **2000**, *97*, 11244–11249.
- (15) Plumeyers, W.; Neamati, N.; Pannecouque, C.; Fikkert, V.; Marchand, C.; Burke, T. R.; Pommier, Y.; Schols, D.; DeClercq, E.; Debyser, Z.; Witvrouw, M. Viral entry as the primary target for the anti-HIV activity of chioric acid and its tetra-acetyl esters. *Mol. Pharmacol.* **2000**, *58*, 641–648.

- (16) Vandegraaff, N.; Kumar, R.; Hocking, H.; Burke, T. R., Jr.; Mills, J.; Rhodes, D.; Burrell, C. J.; Li, P. Specific inhibition of human immunodeficiency virus type 1 (HIV-1) integration in cell culture: putative inhibitors of HIV-1 integrase. *Antimicrob. Agents Chemother.* **2001**, *45*, 2510–2516.
- (17) Pluymers, W.; Pais, G.; Neamati, N.; Pannecouque, C.; Fikkert, V.; Pommier, Y.; Clercq, E. D.; Witvrouw, M.; Burke, T. R., Jr.; Debyser, Z. Inhibition of HIV-1 integrase activity and HIV-1 replication by a series of diketo derivatives. *Mol. Pharmacol.*, in review.
- (18) Hazuda, D. J.; Felock, P.; Witmer, M.; Wolfe, A.; Stillmock, K.; Grobler, J. A.; Espeseth, A.; Gabryelski, L.; Schleif, W.; Blau, C.; Miller, M. D. Inhibitors of strand transfer that prevent integration and inhibit HIV-1 replication in cells. *Science* **2000**, *287*, 646–650.
- (19) Marchand, C.; Zhang, X.; Pais, G. C. G.; Cowsansage, K.; Neamati, N.; Burke, T. R., Jr.; Pommier, Y. Structural determinants for HIV-1 integrase inhibition by β -diketo acids. *J. Biol. Chem.* **2002**, *277*, 12596–12603.
- (20) Neamati, N. Structure-based HIV-1 integrase inhibitor design: a future perspective. *Expert Opin. Invest. Drugs* **2001**, *10*, 281–296.
- (21) Neamati, N.; Marchand, C.; Winslow, H. E.; Pommier, Y. Human immunodeficiency virus type 1 integrase-targeted inhibitor design. *Antiretroviral Ther.* **2001**, *87*–104.
- (22) Young, S. D. Inhibition of HIV-1 integrase by small molecules: the potential for a new class of AIDS chemotherapeutics. *Curr. Opin. Drug Discovery Dev.* **2001**, *4*, 402–410.
- (23) Wai, J. S.; Egbertson, M. S.; Payne, L. S.; Fisher, T. E.; Embrey, M. W.; Tran, L. O.; Melamed, J. Y.; Langford, H. M.; Guare, J. P., Jr.; Zhuang, L.; Grey, V. E.; Vacc, J. P.; Holloway, M. K.; Naylor-Olsen, A. M.; Hazuda, D. J.; Felock, P. J.; Wolfe, A. L.; Stillmock, K. A.; Schleif, W. A.; Gabryelski, L. J.; Young, S. D. 4-Aryl-2,4-dioxobutanoic acid inhibitors of HIV-1 integrase and viral replication in cells. *J. Med. Chem.* **2000**, *43*, 4923–4926.
- (24) Fujishita, T.; Yoshinaga, T.; Yamauchi, H. (Shionogi & Co., Ltd.). Indole derivatives with antiviral activity. PCT Int. Appl. WO-9950245, 1999.
- (25) Barrett, C. B.; Beer, R. J. S.; Dodd, G. M.; Robertson, A. The chemistry of Bacteria. Part VI. The synthesis of a trimethyl derivative of the C20 acid from Violacein. *J. Chem. Soc.* **1957**, 4810–4813.
- (26) Klaubert, D. H.; Sellstedt, J. H.; Guinasso, C. J.; Bell, S. C.; Capetola, R. J. 5-Tetrazolecarboxamides and their salts: new orally active antiallergy agents. *J. Med. Chem.* **1981**, *24*, 748–752.
- (27) Tang, Y.; Nicklaus, M. C. Refined model of the HIV-1 integrase-viral DNA complex used for inhibitor docking studies. Presented at the 222nd ACS National Meeting of the American Chemical Society, Chicago, IL, Aug 26–30, 2001.
- (28) Brautigam, C. A.; Steitz, T. A. Structural and functional insights provided by crystal structures of DNA polymerases and their substrate complexes. *Curr. Opin. Struct. Biol.* **1998**, *8*, 54–63.
- (29) Thornber, C. W. Isosterism and molecular modification in drug design. *Chem. Soc. Rev.* **1979**, *8*, 563–580.
- (30) Patani, G. A.; LaVoie, E. J. Bioisosterism: A rational approach in drug design. *Chem. Rev.* **1996**, *96*, 3147–3176.
- (31) Marchand, C.; Neamati, N.; Pommier, Y. In vitro human immunodeficiency virus type 1 integrase assays. *Methods Enzymol.* **2001**, *340*, 624–633.
- (32) SYBYL 6.7.1; S. Tripos Inc.: St. Louis, MO, 2001.
- (33) Tang, Y.; Nicklaus, M. C. Molecular modeling of full-length HIV-1 integrase and its complexes with viral and human DNA. Presented at the 221st ACS National Meeting of the American Chemical Society, San Diego, CA, Apr 1–5, 2001.
- (34) *Gaussian 98*; G. Gaussian Inc.: Pittsburgh, PA, 1998.
- (35) Rarey, M.; Kramer, B.; Lengauer, T.; Klebe, G. A fast flexible docking method using an incremental construction algorithm. *J. Mol. Biol.* **1996**, *261*, 470–489.
- (36) Brooks, B. R.; Brucoleri, R. E.; Olafson, B. D.; States, D. J.; Swaminathan, S.; Karplus, M. Charmm – a Program for Macromolecular Energy, Minimization, and Dynamics Calculations. *J. Comput. Chem.* **1983**, *4*, 187–217.
- (37) MacKerell, A. D.; Bashford, D.; Bellott, M.; Dunbrack, R. L.; Evanseck, J. D.; Field, M. J.; Fischer, S.; Gao, J.; Guo, H.; Ha, S.; Joseph-McCarthy, D.; Kuchnir, L.; Kucsera, K.; Lau, F. T. K.; Mattos, C.; Michnick, S.; Ngo, T.; Nguyen, D. T.; Prodhom, B.; Reiher, W. E.; Roux, B.; Schlenkrich, M.; Smith, J. C.; Stote, R.; Straub, J.; Watanabe, M.; Wiorkiewicz-Kuczera, J.; Yin, D.; Karplus, M. All-atom empirical potential for molecular modeling and dynamics studies of proteins. *J. Phys. Chem. B* **1998**, *102*, 3586–3616.
- (38) Foloppe, N.; MacKerell, A. D. All-atom empirical force field for nucleic acids: I. Parameter optimization based on small molecule and condensed phase macromolecular target data. *J. Comput. Chem.* **2000**, *21*, 86–104.
- (39) This study utilized the high-performance computational capabilities of the SGI Origin 2000 system and the Biowulf/LoBoS3 cluster at the Center for Information Technology, National Institutes of Health, Bethesda, MD.
- (40) *Quanta/CHARMM 2000 and InsightII 2000*; Accelrys Inc.: San Diego, CA, 2000.
- (41) Flynn, D. L.; Belliotti, T. R.; Bector, A. M.; Connor, D. T.; Kostlan, C. R.; Nies, D. E.; Ortwine, D. F.; Schrier, D. J.; Sircar, J. J. Styrylpyrazoles, styrylisoxazoles, and styrylisothiazoles – novel 5 lipoxygenase and cyclooxygenase inhibitors. *J. Med. Chem.* **1991**, *34*, 518–525.
- (42) Andreichikov, Y. S.; Maslivets, A. N.; Smirnova, L. I.; Krasnykh, O. P.; Kozlov, A. P.; Perevozchikov, L. A. Five-member 2,3-dioxoheterocycles. 5. Synthesis of 1-aryl-4-aryl-5-methoxycarbonyl-2,3-dihydro-2,3-pyrrolediones – Their interaction with water and alcohols. *Zh. Org. Khim.* **1987**, *23*, 1534–1543.
- (43) Fontana, F.; Minisci, F.; Barbosa, M. C. N.; Vismara, E. Homolytic acylation of protonated pyridines and pyrazines with alpha-keto acids – the problem of monoacylation. *J. Org. Chem.* **1991**, *56*, 2866–2869.
- (44) Caronna, T.; Fronza, G.; Minisci, F.; Porta, O. Homolytic acylation of protonated pyridine and pyrazine derivatives. *J. Chem. Soc., Perkin Trans. 2* **1972**, 2035–2038.
- (45) El-Bahaie, S.; Assy, M. G.; Hassanien, M. M. Synthesis and biological activity of some azoles and azines. *J. Indian Chem. Soc.* **1990**, *67*, 757–758.
- (46) Ketcha, D. M.; Gribble, G. W. A convenient synthesis of 3-acylindoles via friedel-crafts acylation of 1-(phenylsulfonyl)indole – A new route to pyridocarbazole-5,11-quinones and ellipticine. *J. Org. Chem.* **1985**, *50*, 5451–5457.
- (47) Boger, D. L.; Ledebner, M. W.; Kume, M.; Searcey, M.; Jin, Q. Total synthesis and comparative evaluation of luzopeptin A–C and quinoxapeptin A–C. *J. Am. Chem. Soc.* **1999**, *121*, 11375–11383.
- (48) Jacobs, R. T.; Brown, F. J.; Cronk, L. A.; Aharony, D.; Buckner, C. K.; Kusner, E. J.; Kirkland, K. M.; Neilson, K. L. Substituted 3-(phenylmethyl)-1H-indole-5-carboxamides and 1-(phenylmethyl)indole-6-carboxamides as potent, selective, orally active antagonists of the peptidoleukotrienes. *J. Med. Chem.* **1993**, *36*, 394–409.

JM020037P